

**THE EFFECT OF UV SURFACE FLUX SHIELDING BY SPACECRAFT GEOMETRIES.** Christina L. Smith<sup>1\*</sup>, John E. Moores<sup>1</sup> and Andrew C. Schuerger<sup>2</sup> <sup>1</sup>York University, 4700 Keele Street, Toronto, ON, M3J 1P3, <sup>2</sup>University of Florida, Space Life Sciences Lab, 505 Odyssey Way, N. Merritt Island, FL 32953.  
\*Email: chrsmith@yorku.ca

**Introduction:** Ultraviolet radiation reaching the surface of Mars undergoes significantly less attenuation by the atmosphere than is found on Earth due to the lower abundance of ozone and lower atmospheric pressure (e.g. [1]). UV radiation can affect surface chemistry, including the degradation of organic compounds, and has a significant effect on the habitability of the surface of Mars. The effects of small-scale surface geometry shielding (e.g. overhangs, pits) on the Martian surface UV flux have previously been studied [2], but the effects of spacecraft geometries on the incident UV flux at the surface had yet to be investigated. In this paper, we describe a model and method used to examine the effect of idealized spacecraft geometries on the UV flux received by the ground in the component's vicinity, considering both shadowing and reflections.

**Model description:** This work has been carried out using the Doubling and Adding (D&A) radiative transfer code of [3], adapted for Mars. This code is based upon the doubling and adding method of [4]. The ground is assumed to be a Hapke surface with parameters:  $b_0=0.8$ ,  $h=0.06$ ,  $c=0.45$ ,  $b=0.30$  [5]. The surface pressure is assumed to be 6.1mbar. The model is currently being operated in a 2-level, 1-layer approximation although investigations into the effect of multiple layers are underway. The model outputs both a direct and a diffuse component of downward flux.

**Optical depth contribution due to gases:** The optical depth due to Rayleigh scattering,  $\tau_R$ , for a given gas species as a function of pressure,  $P$ , and wavelength,  $\lambda$ , in the UV has been calculated, using the method of [6]:

$$\tau_R = \frac{P \sigma}{g \mu} = \frac{P}{g \mu} \frac{(6+3\delta)}{(6-7\delta)} \frac{8\pi^3}{3N^2\lambda^4} (n_g^2 - 1)^2$$

where  $g$  is the surface gravity of the planet,  $3.71 \text{ ms}^{-2}$ ,  $\mu$  is the mean molecular mass of the gas in question,  $\sigma$  is the Rayleigh scattering coefficient as a function of wavelength,  $n_g$  is the refractive index as a function of wavelength, taken from Allen's Astrophysical

Quantities (4<sup>th</sup> ed.),  $N$  is Lorschmidt's number if the refractive index used was obtained at STP, as in this work, and  $\delta$  is the depolarization parameter, taken from [6] or [7] when not available in the former. The total optical depth due to Rayleigh scattering,  $\tau_{Rtot}$ , from all species is therefore:

$$\tau_{Rtot} = \sum_i \tau_{R,i} f_i$$

where  $f_i$  is the mixing ratio of species  $i$ .

Gaseous absorption of many of the constituent species of the Mars model is negligible at certain wavelengths, depending on the species in question. When non-negligible, the optical depth due to gaseous absorption has been computed using the relevant absorption cross-sections taken from the literature, and is excluded from the model when the effect would be negligible.

**Optical depth contribution due to aerosols:** The aerosol particles are assumed to be spherical mie particles with parameters taken from [5] and [8] (e.g.  $A=1.6$ ,  $B=0.27$ ,  $AMU1=1.493$ ,  $AMU2=0.0170$ ).

**Model validation:** The model was validated by comparing the results from this work to that of the well-tested model of [5]. Their figure 2 shows the total flux received by a UVA receiver on the surface of Mars as a function of aerosol optical depth. The parameters of

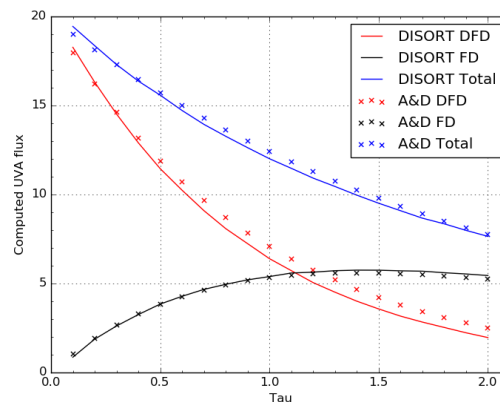


Figure 1: comparison of computed received UVA flux ( $W/m^2$ ) from this work (crosses) with that of [5] (lines).

our model were identical to those of [5] as far as possible. The incident Solar flux at the top of the atmosphere was assumed to be  $20.0 \text{ W/m}^2$ . The results of this are shown in Fig 1. The total results closely match that of [5], despite a slightly higher direct downward flux in our model.

**Idealised spacecraft reflection and shadowing:** The spacecraft components are considered to be idealised geometric shapes – e.g. plates, cubes, oblongs and cylinders. The effects of shadowing build upon the work used to simulate shadowing of rock cracks on Mars, described in [9]. This takes the outputted atmospheric flux maps from the D&A code and casts shadows from each point in the atmosphere, assuming that each point emits a parallel vector field with direction described by the azimuth and zenith angles of the atmospheric point in question and with an intensity equal to the flux of that point within the D&A atmospheric flux map. Where a shadow is cast by a given vector field, the ground in shadow is assumed to receive zero energy, and the regions not in shadow receive 100% of the available energy (corrected by the dot product of the normal surface vector and incident insolation vector). This is repeated for every grid point in the atmospheric map and the received flux on the

ground summed, giving the received flux for an instance in time. This can be repeated over a specific time frame (e.g. one sol, one year) to give the total received insolation over that time period. The reflection component adapts the internal reflection method used in [10] to simulate self-illumination of penitentes on Pluto. This assumes a uniform albedo of the spacecraft component and a uniform reflection of the received energy.

**UV flux maps:** An example flux map for a flat, square plate raised off the ground with no reflection in the UVA band alone is shown in Figure 2. The plate is parallel to the surface and raised off the ground by a height of 0.25 times the length of one of the sides of the plate. The relative intensity of the UV flux is shown in the colorbar. There are 100 time-points in the simulated sol and the sun travels from east to west almost directly overhead. North is in the positive x direction.

The computation of maps of UV flux (in multiple UV bands) over a variety of time periods and in the vicinity of more complex idealised spacecraft components are ongoing, and the results will be available prior to the Lunar and Planetary Sciences Conference 2017.

**Acknowledgements:** CLS would like to acknowledge L. Doose for discussions concerning the D&A model.

**References:** [1] Cockell et al., 2000, *Icarus* 146, 343–359; [2] Moores et al., 2007, *Icarus* 192, 417–433; [3] Griffiths et al., 2012, *Icarus*, 218, 975–988; [4] Hansen, J.E., 1971. *J. Atmos. Sci.* 28, 120–125; [5] Smith M. et al., 2016 *Icarus* 280, p. 234–248; [6] Hansen, J.E., and Travis, L.D., 1974, *SSR*, 16, 527–610; [7] Penndorf, R., 1957, *JOSA*, 47, 176–182; [8] Wolff et al., 2010, *Icarus* 208, 143–155; [9] Smith, C. L. & Moores, J. E., 2015, *LPI Contribution No.* 1903, p.1644; [10] Moores et al., 2017, *Nature*, doi:10.1038/nature20779.

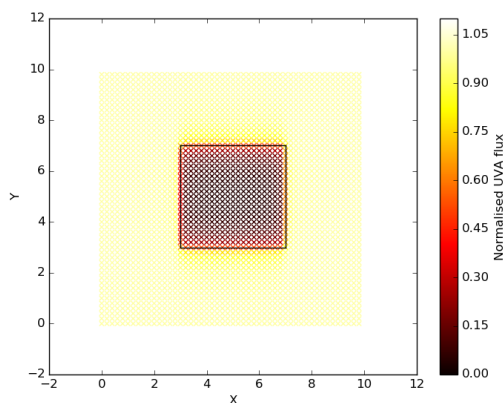


Figure 2: Map of UVA flux received by the ground, normalised to the maximum received, in the vicinity of a flat plate raised above the ground. The position and size of the plate are indicated by the black outlines.